Hindawi
International Journal of Aerospace Engineering
Volume 2019, Article ID 2016416, 10 pages
https://doi.org/10.1155/2019/2016416

Research Article

Robust Integral Terminal Sliding Mode Control for Quadrotor UAV with External Disturbances

Moussa Labbadi and Mohamed Cherkaoui

Engineering for Smart and Sustainable Systems Research Center, Mohammadia School of Engineers, Mohammed V University in Rabat, Morocco

Correspondence should be addressed to Moussa Labbadi; moussalabbadi@research.emi.ac.ma

Received 23 March 2019; Revised 20 June 2019; Accepted 13 July 2019; Published 19 August 2019

Academic Editor: Antonio Concilio

The purpose of this paper is to solve the problem of controlling of the quadrotor exposed to external constant disturbances. The quadrotor system is partitioned into two parts: the attitude subsystem and the position subsystem. A new robust integral terminal sliding mode control law (RITSMC) is designed for stabilizing the inner loop and the quick tracking of the right desired values of the Euler angles. To estimate the disturbance displayed on the z-axis and to control the altitude position subsystem, an adaptive backstepping technique is proposed, while the horizontal position subsystem is controlled using the backstepping approach. The stability of the quadrotor subsystems is guaranteed by the Lyapunov theory. The effectiveness of the proposed methods is clearly comprehended through the obtained results of the various simulations effectuated on MATLAB/Simulink, and a comparison with another technique is presented.

1. Introduction

1.1. Background and Motivation. Over the last decade, the robotic field has attracted great attention from researchers, in particular, the unmanned aerial vehicle (UAV). The quadrotor is a type of drone, which consists of four rotors. This last has a simple mechanical structure. The quadrotor can land vertically and take off. The quadrotor has been used in many applications such as military missions, journalism, disaster management, archaeology, geographical monitoring, taxi services, search/rescue missions, environmental protection, performing missions in oceans or other planets, mailing and delivery, and other miscellaneous applications [1, 2]. Therefore, the quadrotor is a strongly coupled and highly nonlinear system. The quadrotor is an underactuated system, because the six DOF (x, y, z, ϕ, θ, and ψ) should be regulated by the four controls.

In order to control the quadrotor in a closed loop, many techniques have been designed such as the backstepping control, fuzzy logic based on intelligent control, sliding mode control, adaptive control approaches, neural network method, intelligent fuzzy logic control, model predictive control [3], hybrid finite-time control [4], proportional derivative sliding mode control [5], nonlinear PID controller [6], and adaptive fractional order sliding mode control [7].

1.2. Literature Review. In Reference [8], nonlinear control techniques are designed for the quadrotor's position and attitude. The attitude loop uses the regular sliding mode controller. The backstepping technique is combined with a sliding mode control to design robust controllers for the outer loop and the yaw angle. In order to estimate the quadrotor UAV fault, an observer is developed. In Reference [9], a second-order sliding mode control technique is developed to control an underactuated quadrotor UAV. In order to select the best coefficient of this proposed controller, the Hurwitz analysis is used. The control approach allows converging the state variables to their reference values and ensuring the stability of the quadrotor system. In Reference [10], a global fast terminal sliding mode control technique is developed for a quadrotor UAV. The controller allows solving the chattering problem, stabilizing the vehicle, and converging all state variables to zero. In Reference [11], a nonsingular fast terminal SMC technique has been established for the stabilization and

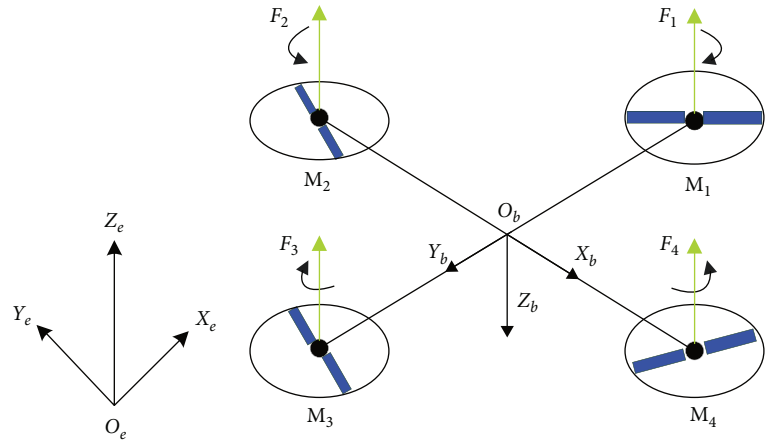

Figure 1: The quadrotor UAV with four rotors.

control of uncertain and nonlinear dynamical systems based on a disturbance observer. In Reference [12], an adaptive control method based on the sliding mode technique is developed for tracking control and for the stability of an uncertain quadrotor. The quadrotor unknown parameters are estimated at any moment. The proposed control laws guarantee the stability of the quadrotor system and recommend that the state variables converge to their origin values in finite time. A combination of sliding mode control and integral backstepping techniques is presented in Reference [13]. The control strategy allows tracking of the flight trajectory in the presence of the disturbances and stabilizing of the attitude of the UAV. In Reference [14], a nonsingular fast terminal sliding mode (NFTSM) method is designed to obtain the good performance of the quadrotor attitude. The tracking errors of the quadrotor are converged to zero through this controller. In the study by Reference [15], a fast terminal SMC approach is proposed for the tracking control problem of a nonlinear mass-spring system in the presence of noise, exterior disturbance, and parametric uncertainty. The proposed controller is confirmed via both experimental and simulation results. In Reference [16], a high-order sliding mode observer is combined with a nonsingular modified super-twisting algorithm to propose a solution for the trajectory-tracking problem of unmanned aerial systems (UAS). The proposed approach techniques offer an estimation for the translational velocities of the quadrotor and improve the robust performance ability of the UAV system against external disturbances. In Reference [17], an adaptive super-twisting based on the terminal sliding mode technique is applied on the fourth-order systems. The experimental results of the proposed control scheme are presented. In Reference [18], a terminal sliding mode controller for the yaw and altitude subsystems is designed. A sliding mode technique is developed to control the quadrotor underactuated subsystem. In Reference [19], two nonlinear control techniques (backstepping and sliding mode controllers) are suggested to solve the tracking trajectory problem in the presence of relatively high perturbations, problems of the quadrotor system affected by input delays, parametric uncertainties, unmolded uncertainties, and time-varying state and external disturbances; a robust nominal controller and a robust compensator are proposed in Reference [20] to solve the process.

1.3. Contribution. In this paper, a robust integral terminal sliding mode control method is proposed for a quadrotor attitude. Then, an integral terminal sliding mode surface is used for the attitude of the quadrotor to ensure tracking errors converge to zero in short finite time. The RITSMC scheme is designed based on the Lyapunov theory. However, an adaptive backstepping is designed to estimate the unknown external disturbance acting in the z-axis and to control the altitude subsystem. The backstepping technique is used to control the horizontal position of the quadrotor in the presence of external perturbations. The contribution of this paper is given by the following points:

(i) A novel hybrid control structure of the quadrotor system subject to underactuated, kinematics-dynamics couplings, and external disturbances is proposed

(ii) An RITSMC is proposed for the quadrotor attitude to eliminate singularities without adding any constraints compared to TSMC and to reduce the chattering effect in the conventional SMC

(iii) An AB control approach commands the altitude of the quadrotor and estimates the disturbances at any moment simultaneously

1.4. Paper Organization. The rest of the paper is structured as follows: the formulation of the quadrotor system is given in Section 2. The new RITSMC and the adaptive backstepping techniques are presented in Section 3. The numerical simulation results are prepared in Section 4. Finally, the conclusions are exposed in Section 5.

2. The System Modeling

The quadrotor is equipped with four rotors as shown in Figure 1. The body-fixed (O_b, X_b, Y_b, and Z_b) and earth-fixed (O_e, X_e, Y_e, and Z_e) frames are defined. The absolute position of the quadrotor is defined by the vector $\xi =$

$[x, y, z]^T$. The vector $\eta = [\phi, \theta, \psi]^T$ represents the Euler angles. The angular and linear velocities of the quadrotor are defined by the vectors $\Omega = [p, q, r]^T$ and $V = [u, v, w]^T$, respectively.

In this context, the formalism of Newton-Euler is used to obtain the quadrotor model [19, 21, 22]:

$$\begin{cases} \dot{\xi} = V, \\ m\dot{V} = R\,F\,e_3 - mge_3 - k_i \quad (i = 1, 2, 3), \\ \dot{R} = RS(\Omega), \\ J\dot{\Omega} = -\Omega \times J\,\Omega + M_c - M_a + M_b. \end{cases} \tag{1}$$

R is the rotation matrix

$$R = \begin{bmatrix} C_\theta\,C_\psi & S_\phi\,S_\theta C_\psi - C_\theta\,S_\psi & C_\phi\,S_\theta C_\psi + S_\phi\,S_\psi \\ C_\theta\,S_\psi & S_\phi\,C_\theta S_\psi + C_\phi\,S_\psi & C_\phi\,S_\theta S_\psi - S_\phi\,C_\psi \\ -S_\theta & C_\phi\,C_\theta & C_\phi\,C_\theta \end{bmatrix}. \tag{2}$$

The coordinate transformation is given by the rotation matrix:

$$T = \begin{bmatrix} 1 & 0 & -S_\theta \\ 0 & C_\phi & S_\phi\,C_\theta \\ 0 & -S_\phi & C_\phi\,C_\theta \end{bmatrix}. \tag{3}$$

We use $C(.)$ to cos $(.)$ and $S(.)$ to sin $(.)$. m represents the total mass of the quadrotor, $I_{3\times3}$ is a density matrix, and $J = \text{diag}\ (I_x, I_y, I_z)$ denotes the matrix moment of the inertia. F is the total thrust; this expression is given by $F = F_1 + F_2 + F_3 + F_4$ where $F_i = b\Omega_i^{\,2}$, Ω_i is the angular speed and b is a parameter that depends on the air density and blade geometry. $S = [p, q, r]^T$ denotes a skew-symmetric matrix. M_a, M_c, and M_a are the resultant of the aerodynamic friction torque, the resultant of the gyroscopic effect torque, and the torque developed by the four rotors of the quadrotor, respectively. These expressions can be given, respectively, as follows:

$$M_a = \text{diad}\left(k_4\dot{\phi}^2, k_5\dot{\theta}^2, k_6\dot{\psi}^2\right), \tag{4}$$

where k_4, k_5, and k_6 represent the friction aerodynamics parameters.

$$M_c = \sum_{i=0}^{4} \Omega \times J_r\left[0, 0, (-1)^{i+1}\Omega_i\right]^T. \tag{5}$$

J_r denotes the rotor inertia.

$$M_b = \begin{bmatrix} l(F_3 - F_1) \\ l(F_4 - F_2) \\ d(-\Omega_1 + \Omega_2 - \Omega_3 + \Omega_4) \end{bmatrix}, \tag{6}$$

d is the drag coefficient and l is the distance between a propeller and the center of the quadrotor. The complete quadrotor dynamics in the presence of external disturbances referred to in [22] is as

$$\begin{cases} \ddot{\phi} = \dot{\theta}\dot{\psi}\dfrac{I_y - I_z}{I_x} - \dot{\theta}\dfrac{J_r}{I_x}\Omega_r - \dfrac{k_4}{I_x}\dot{\phi}^2 + \dfrac{1}{I_x}U_2 + d_\phi, \\ \ddot{\theta} = \dot{\phi}\dot{\psi}\dfrac{I_z - I_x}{I_y} + \dot{\phi}\dfrac{J_r}{I_y}\Omega_r - \dfrac{k_5}{I_y}\dot{\theta}^2 + \dfrac{1}{I_y}U_3 + d_\theta, \\ \ddot{\psi} = \dot{\phi}\dot{\theta}\dfrac{I_x - I_y}{I_z} - \dfrac{k_6}{I_z}\dot{\psi}^2 + \dfrac{1}{I_z}U_4 + d_\psi, \\ \ddot{x} = \dfrac{1}{m}\left(\left(C_\phi S_\theta C_\psi + S_\phi\,S_\psi\right)U_1 + d_x\right) - \dfrac{k_1}{m}\dot{x}, \\ \ddot{y} = \dfrac{1}{m}\left(\left(C_\phi S_\theta S_\psi - S_\phi\,C_\psi\right)U_1 + d_y\right) - \dfrac{k_2}{m}\dot{y}, \\ \ddot{z} = \dfrac{1}{m}\left(C_\phi C_\theta U_1 + d_z\right) - g - \dfrac{k_3}{m}\dot{z}. \end{cases} \tag{7}$$

The relationship between the quadrotor inputs and the propeller speeds of the quadrotor can be written as follows [22]:

$$\begin{bmatrix} U_1 \\ U_2 \\ U_3 \\ U_4 \end{bmatrix} = \begin{bmatrix} b & b & b & b \\ -lb & 0 & lb & 0 \\ 0 & -lb & 0 & lb \\ -d & +d & -d & d \end{bmatrix} \begin{bmatrix} \Omega_1^2 \\ \Omega_2^2 \\ \Omega_3^2 \\ \Omega_4^2 \end{bmatrix}. \tag{8}$$

The dynamic model of the quadrotor position subsystem has three outputs (z, x, and y) and one control input U_1. In order to solve the underactuated problem, three virtual control (v_1, v_2, and v_3) inputs using adaptive backstepping and the backstepping technique are designed. The virtual control inputs are given as follows:

$$\begin{bmatrix} v_1 \\ v_2 \\ v_3 \end{bmatrix} = \begin{bmatrix} \dfrac{U_1}{m}\left(C_\phi S_\theta C_\psi + S_\phi S_\psi\right) \\ \dfrac{U_1}{m}\left(C_\phi S_\theta S_\psi - S_\phi C_\psi\right) \\ \dfrac{U_1}{m}\left(C_\phi C_\theta\right) - g \end{bmatrix}. \tag{9}$$

Therefore, the desired roll, pitch, and yaw angles (ϕ_d, θ_d) and the total thrust U_1 can be obtained as follows:

$$\begin{cases} U_1 = m\sqrt{{v_1}^2 + {v_2}^2 + (v_3 + g)^2}, \\ \phi_d = \arctan\left[S_{\theta d}\left(\dfrac{v_1 C_{\psi d} - v_2 S_{\psi d}}{v_3 + g}\right)\right], \\ \theta_d = \arctan\left(\dfrac{v_1 C_{\psi d} + v_2 S_{\psi d}}{(v_3 + g)}\right). \end{cases} \tag{10}$$

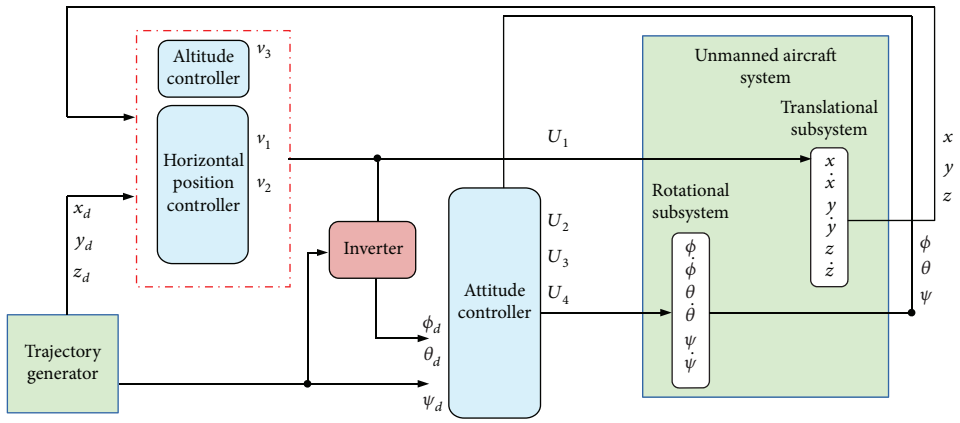

Figure 2: The control general structure for the quadrotor UAV.

3. Controller Design and Stability Analysis

This section presents the robust nonlinear controller for the quadrotor UAV in the presence of external perturbations. The proposed control of the quadrotor is divided into the inner loop and the outer loop. For the outer loop, an adaptive backstepping (AB) controller for the altitude subsystem is designed. The AB method ensures the tracking of the desired altitude z_d and an accurate estimation of the unknown perturbation d_z acting on the altitude subsystem. The backstepping technique is used to obtain the virtual control (v_1, v_2). For the inner loop, a new robust integral terminal sliding mode control (RITSMC) is proposed. The attitude controller generates the rolling, pitching, and yawing torques to control the orientation of the quadrotor in the presence of external disturbances. Finally, the proposed control strategy solves the trajectory problem in short finite time with accuracy of the system performance. The general proposed control scheme is shown in Figure 2.

3.1. Adaptive Backstepping Control for Altitude Subsystem. Define tracking error of the altitude subsystem as

$$e_{z1} = z - z_d. \tag{11}$$

Consider the Lyapunov candidate function:

$$V_{z1} = \frac{1}{2} e_{z1}^2. \tag{12}$$

Taking the time derivative of equation (12)

$$\dot{V}_{z1} = e_{z1}\dot{e}_{z1} = e_{z1}(\dot{z} - \dot{z}_d). \tag{13}$$

The virtual control law is

$$\alpha_z = -c_{z1}e_{z1} + \dot{z}_d, \tag{14}$$

where $c_{z1} > 0$ is a positive constant.

Define the tracking error of step 2 as

$$e_{z2} = \dot{z} - \alpha_z. \tag{15}$$

The virtual control and adaptive law of the altitude subsystem are given by equation (16) and equation (17), respectively:

$$v_3 = -\left(e_{z1} + c_{z1}(e_{z2} - cz1e_{z1}) + c_{z2}e_{z2} + \frac{k_3}{m}\dot{z} - \ddot{z}_d + \hat{d}_z\right), \tag{16}$$

$$\dot{\hat{d}}_z = \gamma_z e_{z2}, \tag{17}$$

where c_{z2} and γ_z are the positive parameters and $\hat{d}_z$ denotes the estimate of d_z.

Proof. The Lyapunov function is considered as follows:

$$V_{z2} = \frac{1}{2}{e_{z1}}^2 + \frac{1}{2}{e_{z2}}^2 + \frac{1}{2\gamma_z}{\tilde{d}_z}^2. \tag{18}$$

The time derivative of V_{z2} is given as

$$\begin{aligned}\dot{V}_{z2} &= e_{z1}\dot{e}_{z1} + e_{z2}\dot{e}_{z2} + \frac{1}{\gamma_z}\dot{\tilde{d}}_z\tilde{d}_z \\ &= e_{z1}(e_{z2} - c_{z1}e_{z1}) + e_{z2}(\ddot{z} + c_{z1}\dot{e}_{z1} - \ddot{z}_d) - \frac{1}{\gamma_z}\dot{\hat{d}}_z\tilde{d}_z \\ &= -c_{z1}e_{z1}^2 + e_{z2}\left[-\frac{k_3}{m}z + v_3 + c_{z1}(e_{z2} - c_{z1}e_{z1}) - \ddot{z}_d\right] \\ &\quad + e_{z2}\hat{d}_z + d_z\left(e_{z2} - \frac{\dot{\hat{d}}_z}{\gamma_z}\right).\end{aligned} \tag{19}$$

Considering the control law equation (16) and adaptive law equation (17), we get

$$\dot{V}_{z2} = -c_{z1}e_{z1}^2 - c_{z2}e_{z2}^2 \le 0. \tag{20}$$

3.2. Backstepping Control for Horizontal Position Subsystem. In this part, the backstepping technique is used to control the horizontal position of a quadrotor.

Introduce the tracking errors of the x and y positions:

$$\begin{aligned}e_{x1} &= x - x_d, \\ e_{y1} &= y - y_d.\end{aligned} \tag{21}$$

Define the Lyapunov candidate function as

$$V_{x1} = \frac{1}{2} {e_{x1}}^2, \tag{22}$$

$$V_{y1} = \frac{1}{2} {e_{y1}}^2. \tag{23}$$

The time derivatives of equations (23) and (24) are given by

$$\dot{V}_{x1} = e_{x1}\dot{e}_{x1} = e_{x1}(\dot{x} - \dot{x}_d), \tag{24}$$

$$\dot{V}_{y1} = e_{y1}\dot{e}_{y1} = e_{y1}(\dot{y} - \dot{y}_d). \tag{25}$$

From equation (25), the virtual control laws are

$$\begin{aligned} \alpha_x &= -c_{x1}e_{x1} + \dot{x}_d, \\ \alpha_y &= -c_{y1}e_{y1} + \dot{y}_d, \end{aligned} \tag{26}$$

where $c_{x1}, c_{y1} > 0$ are the positive constants.

Consider the tracking errors of step 2 are given as

$$\begin{aligned} e_{x2} &= \dot{x} - \alpha_x, \\ e_{y2} &= \dot{y} - \alpha_y. \end{aligned} \tag{27}$$

The virtual control laws of the horizontal subsystems are given by

$$\begin{aligned} v_1 &= -\left(e_{x1} + c_{x1}(e_{x2} - c_{x1}\, e_{x1}) + c_{x2}e_{x2} + \frac{k_1}{m}\dot{x} - \ddot{x}_d + d_x\right), \\ v_2 &= -\left(e_{y1} + c_{y1}\left(e_{y2} - c_{y1}\, e_{y1}\right) + c_{y2}e_{y2} + \frac{k_2}{m}\dot{y} - \ddot{y}_d + d_y\right). \end{aligned} \tag{28}$$

Proof. Using the same, procedure presented in the subsection 3.1 demonstrate the stability of horizontal subsystem.

3.3. Robust Integral Terminal Sliding Mode Control Laws for Attitude Subsystem. In order to solve the chattering phenomenon and to eliminate the singularity in a TSMC, a robust nonlinear controller based on the integral terminal sliding mode technique is designed for the quadrotor attitude.

Introduce the tracking errors and its derivative, respectively, of the attitude subsystem:

$$\begin{cases} e_\phi = \phi - \phi_d, \\ e_\theta = \theta - \theta_d, \\ e_\psi = \psi - \psi_d, \end{cases}$$
$$\begin{cases} \dot{e}_\phi = \dot{\phi} - \dot{\phi}_d, \\ \dot{e}_\theta = \dot{\theta} - \dot{\theta}_d, \\ \dot{e}_\psi = \dot{\psi} - \dot{\psi}_d. \end{cases} \tag{29}$$

Consider the ITSM surface function as of the quadrotor attitude as [23, 24]

$$\begin{cases} s_\phi = \dot{e}_\phi + \int\left(\alpha_\phi \dot{e}_\phi^{\left(q_\phi/p_\phi\right)} + \beta_\phi e_\phi^{\left(q_\phi/\left(2p_\phi - q_\phi\right)\right)}\right)dt, \\ s_\theta = \dot{e}_\theta + \int\left(\alpha_\theta \dot{e}_\theta^{\left(q_\theta/p_\theta\right)} + \beta_\theta e_\theta^{\left(q_\theta/(2p_\theta - q_\theta)\right)}\right)dt, \\ s_\psi = \dot{e}_\psi + \int\left(\alpha_\psi \dot{e}_\psi^{\left(q_\psi/p_\psi\right)} + \beta_\psi\, e_\psi^{\left(q_\psi/\left(2p_\psi - q_\psi\right)\right)}\right)dt, \end{cases} \tag{30}$$

where $\alpha_i (i = \phi, \theta, \psi)$ and $\beta_i (i = \phi, \theta, \psi)$ are the positive constants and $p_i (i = \phi, \theta, \psi)$ and $q_i (i = \phi, \theta, \psi)$ the positive integers with $p_i > q_i$.

The surface dynamics are given by

$$\begin{cases} \dot{s}_\phi = \ddot{e}_\phi + \alpha_\phi \dot{e}_\phi^{\left(q_\phi/p_\phi\right)} + \beta_\phi e_\phi^{\left(q_\phi/\left(2p_\phi - q_\phi\right)\right)}, \\ \dot{s}_\theta = \ddot{e}_\theta + \alpha_\theta \dot{e}_\theta^{(q_\theta/p_\theta)} + \beta_\theta e_\theta^{(q_\theta/(2p_\theta - q_\theta))}, \\ \dot{s}_\psi = \ddot{e}_\psi + \alpha_\psi \dot{e}_\psi^{\left(q_\psi/p_\psi\right)} + \beta_\psi\, e_\psi^{\left(q_\psi/\left(2p_\psi - q_\psi\right)\right)}. \end{cases} \tag{31}$$

Using the exponential reaching laws, we get

$$\begin{cases} \dot{s}_\phi = -\lambda_\phi s_\phi - k_\phi \text{ sign } \left(s_\phi\right), \\ \dot{s}_\theta = -\lambda_\theta s_\theta - k_\theta \text{ sign } \left(s_\theta\right), \\ \dot{s}_\psi = -\lambda_\psi s_\psi - k_\psi \text{ sign } \left(s_\psi\right). \end{cases} \tag{32}$$

From equation (31) and equation (32), the control laws of the attitude subsystem are given as

$$\begin{aligned} U_2 = I_x \Bigg[&-\left(\dot{\theta}\dot{\psi}\frac{I_y - I_z}{I_x} - \dot{\theta}\frac{J_r}{I_x}\,\Omega_r - \frac{k_4}{I_x}\dot{\phi}^2\right) - d_\phi - \lambda_\phi s_\phi \\ &- k_\phi \text{ sign } \left(s_\phi\right) + \ddot{\phi}_d - \alpha_\phi \dot{e}_\phi^{\left(q_\phi/p_\phi\right)} - \beta_\phi e_\phi^{\left(q_\phi/\left(2p_\phi - q_\phi\right)\right)}\Bigg], \\ U_3 = I_y \Bigg[&-\left(\dot{\phi}\dot{\psi}\frac{I_z - I_x}{I_y} + \dot{\phi}\frac{J_r}{I_y}\,\Omega_r - \frac{k_5}{I_y}\dot{\theta}^2\right) - d_\theta - \lambda_\theta s_\theta \\ &- k_\theta \text{ sign } (s_\theta) + \ddot{\theta}_d - \alpha_\theta \dot{e}_\theta^{(q_\theta/p_\theta)} - \beta_\theta e_\theta^{(q_\theta/(2p_\theta - q_\theta))}\Bigg], \\ U_4 = I_z \Bigg[&-\left(\dot{\phi}\dot{\theta}\frac{I_x - I_y}{I_z} - \frac{k_6}{I_z}\dot{\psi}^2\right) - d_\psi - \lambda_\psi s_\psi \\ &- k_\psi \text{ sign } \left(s_\psi\right) + \ddot{\psi}_d - \alpha_\psi \dot{e}_\psi^{\left(q_\psi/p_\psi\right)} - \beta_\psi\, e_\psi^{\left(q_\psi/\left(2p_\psi - q_\psi\right)\right)}\Bigg]. \end{aligned} \tag{33}$$

Proof. In order to demonstrate the stability of the attitude subsystem, the Lyapunov candidate function of the roll subsystem is given as follows:

$$V_\phi = \frac{1}{2} s_\phi^2. \tag{34}$$

Table 1: Quadrotor parameters.

Parameter	Value	Parameter	Value
$g\ (\mathrm{m/s^2})$	9.81	$k_2\ (\mathrm{N/m/s})$	5.567*e*-4
$m\ (\mathrm{kg})$	0.486	$k_3\ (\mathrm{N/m/s})$	6.354*e*-5
$I_x\ (\mathrm{kg\cdot m^2})$	3.827*e*-3	$k_4\ (\mathrm{N/m/s})$	5.567*e*-4
$I_y\ (\mathrm{kg\cdot m^2})$	3.827*e*-3	$k_5\ (\mathrm{N/m/s})$	5.567*e*-4
$I_z\ (\mathrm{kg\cdot m^2})$	7.656*e*-3	$k_6\ (\mathrm{N/m/s})$	6.354*e*-5
$J_r\ (\mathrm{kg\cdot m^2})$	2.838*e*-5	$b\ (\mathrm{N\cdot s^2})$	2.984*e*-3
$k_1\ (\mathrm{N/m/s})$	5.567*e*-4	$d\ (\mathrm{N\cdot m/s^2})$	3.232*e*-2

The time derivative of V_ϕ is

$$\begin{aligned}
\dot{V}_\phi &= s_\phi \dot{s}_\phi = s_\phi \left(\ddot{\phi} - \ddot{\phi}_d + \alpha_\phi \dot{e}_\phi^{\left(q_\phi/p_\phi\right)} + \beta_\phi e_\phi^{\left(q_\phi/\left(2p_\phi - q_\phi\right)\right)} \right) \\
&= s_\phi \left(\dot{\theta}\dot{\psi}\frac{I_y - I_z}{I_x} - \dot{\theta}\frac{J_r}{I_x}\Omega_r - \frac{k_4}{I_x}\dot{\phi}^2 + \frac{1}{I_x}U_2 \right. \\
&\quad \left. + d_\phi - \ddot{\phi}_d + \alpha_\phi \dot{e}_\phi^{\left(q_\phi/p_\phi\right)} + \beta_\phi e_\phi^{\left(q_\phi/\left(2p_\phi - q_\phi\right)\right)} \right) \\
&= s_\phi \left(\dot{\theta}\dot{\psi}\frac{I_y - I_z}{I_x} - \dot{\theta}\frac{J_r}{I_x}\Omega_r - \frac{k_4}{I_x}\dot{\phi}^2 \right. \\
&\quad + \left[-\left(\dot{\theta}\dot{\psi}\frac{I_y - I_z}{I_x} - \dot{\theta}\frac{J_r}{I_x}\Omega_r - \frac{k_4}{I_x}\dot{\phi}^2 \right) - d_\phi - \lambda_\phi s_\phi \right. \\
&\quad \left. \left. - k_\phi\ \mathrm{sign}\left(s_\phi\right) + \ddot{\phi}_d - \alpha_\phi \dot{e}_\phi^{\left(q_\phi/p_\phi\right)} - \beta_\phi e_\phi^{\left(q_\phi/\left(2p_\phi - q_\phi\right)\right)} \right] \right. \\
&\quad \left. + d_\phi - \ddot{\phi}_d + \alpha_\phi \dot{e}_\phi^{\left(q_\phi/p_\phi\right)} + \beta_\phi e_\phi^{\left(q_\phi/\left(2p_\phi - q_\phi\right)\right)} \right) \\
&= s_\phi\left(-\lambda_\phi s_\phi - k_\phi\ \mathrm{sign}\left(s_\phi\right)\right) = -\lambda_\phi {s_\phi}^2 - k_\phi \left|s_\phi\right| \le 0.
\end{aligned} \tag{35}$$

4. Simulation Results

To validate the performances of the proposed controllers, numerical simulations will be presented in this section. The parameters of the quadrotor used in the simulation are selected in Table 1. The initial attitude and position of the quadrotor are chosen as [0, 0, 0] rad and [0, 0, 0] m. The desired trajectory of the yaw angle and the position is given in Table 2. The external disturbances used in the simulation are given as follows: $d_x = 1$ N at $t = 5$ s; $d_\phi = 1$ rad/s^2 at $t = 10$ s; $d_y = 1$ N at $t = 15$ s; $d_\theta = 1$ rad/s^2 at $t = 20$ s; $d_z = 1$ N at $t = 25$ s; and $d_\psi = 1$ rad/s^2 at $t = 30$ s. Besides, the parameters of the proposed controller are listed in Table 3.

Remark 1. In order to achieve a smooth and quick tracking performance, the design parameters of the proposed ABRITSMC, B-SMC, and SMC techniques have been tuned by using a toolbox optimization method in MATLAB/Simulink (see, e.g., [25]).

Table 2: The reference trajectories of the position and yaw angle.

Variables	Value	Time (s)
$[x_d, y_d, z_d]$	[0.6, 0.6, 0.6] m	0
	[0.3, 0.6, 0.6] m	10
	[0.3, 0.3, 0.6] m	20
	[0.6, 0.6, 0.6] m	30
	[0.6, 0.6, 0.6] m	40
	[0.6, 0.6, 0.6] m	50
$[\psi_d]$	[0.5] rad	0
$[\psi_d]$	[0.0] rad	50

Table 3: Control system parameters.

Parameter	Value	Parameter	Value
c_{x1}	1.68	c_{x2}	2.34
c_{y1}	1	c_{y2}	2.25
c_{z1}	6.40	c_{z2}	20
α_i	59.78	β_i	974.57
p_i	54	q_i	52
λ_i	2	k_i	10.66

Furthermore, In order to highlight the superiority of the proposed control laws, comparisons with the backstepping sliding mode control and the first-order sliding mode control technique are done.

The simulation results are shown in Figures 3–8. The desired and actual tracking positions x, y, and z are shown in Figure 3, where the proposed control strategy that drives the quadrotor to track the desired flight trajectory more rapidly and more accurately can be seen, then the classic sliding mode control method and the backstepping sliding mode controller. The constant disturbances are added in the position subsystem at $t = 5$. It appears that the proposed control approach has managed to effectively hold the quadrotor's position in finite time contrary to the SMC and B-SMC; the same behaviour can be observed at $t = 15$ for the y position and at $t = 25$ for the z position of the quadrotor system. Furthermore, trajectory attitudes ϕ, θ, and ψ are shown in Figure 4. It can be seen that the quadrotor attitude tracks the desired angles in short finite time. The attitude sliding variables (s_ϕ, s_θ, and s_ψ) are shown in Figure 6; the convergence to zero in finite time of the sliding surfaces can be observed. The trajectory-tracking errors of the position are depicted in Figure 5. The estimate force acting in direction z is shown in Figure 8. In order to demonstrate the superiority of the proposed control strategy, the quadrotor trajectory path performance in 3-D space is shown in Figure 7. Clearly, it can be seen that the proposed control strategy can accurately track the square trajectory in the presence of external disturbances. The proposed control approach obtains better performance compared to the conventional SMC and B-SMC methods in terms of disturbance rejection and trajectory tracking.

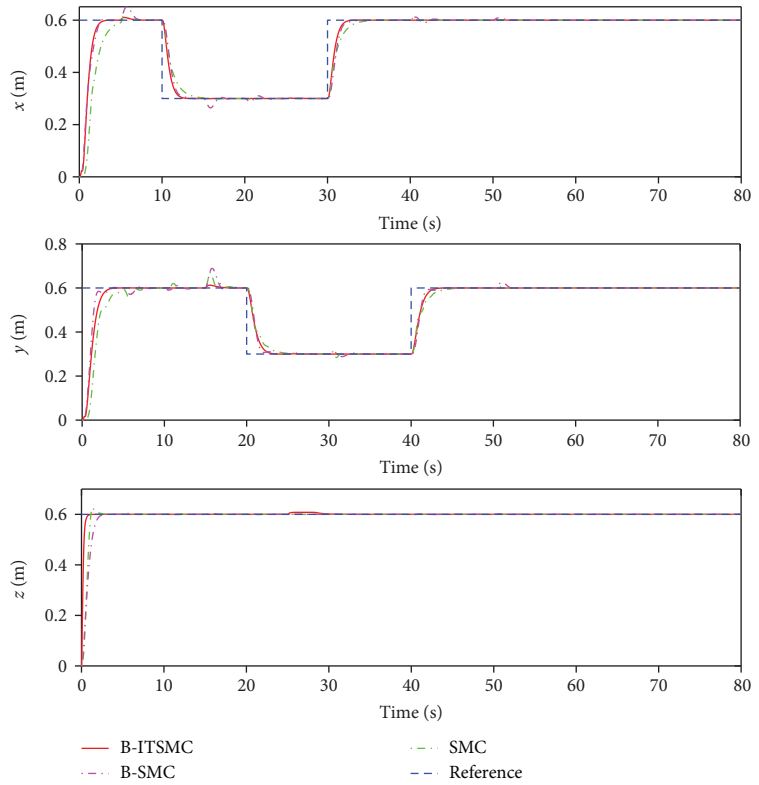

Figure 3: Response of quadrotor position.

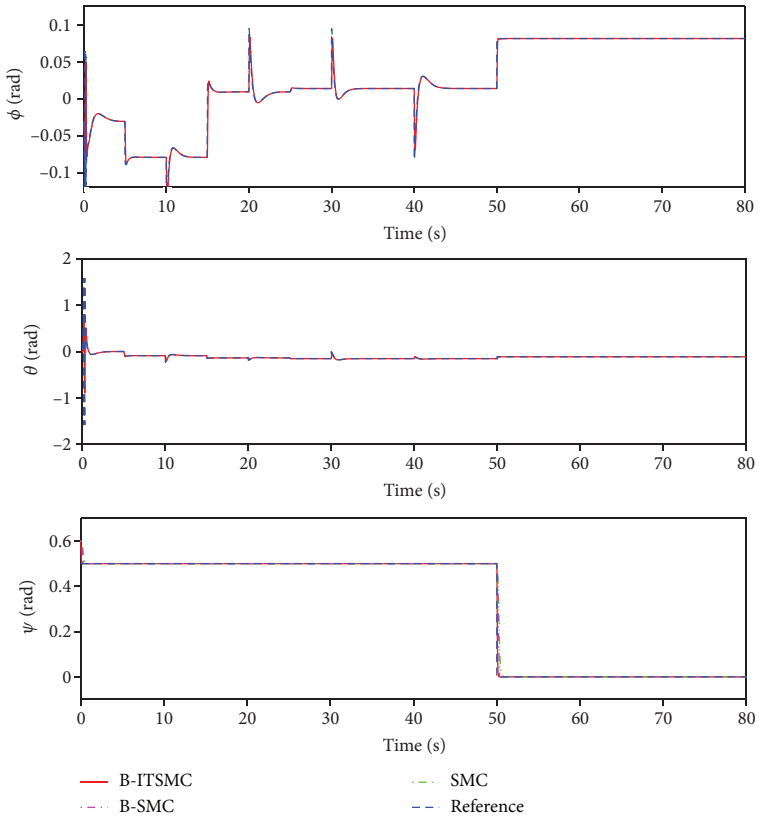

Figure 4: Response of quadrotor attitude.

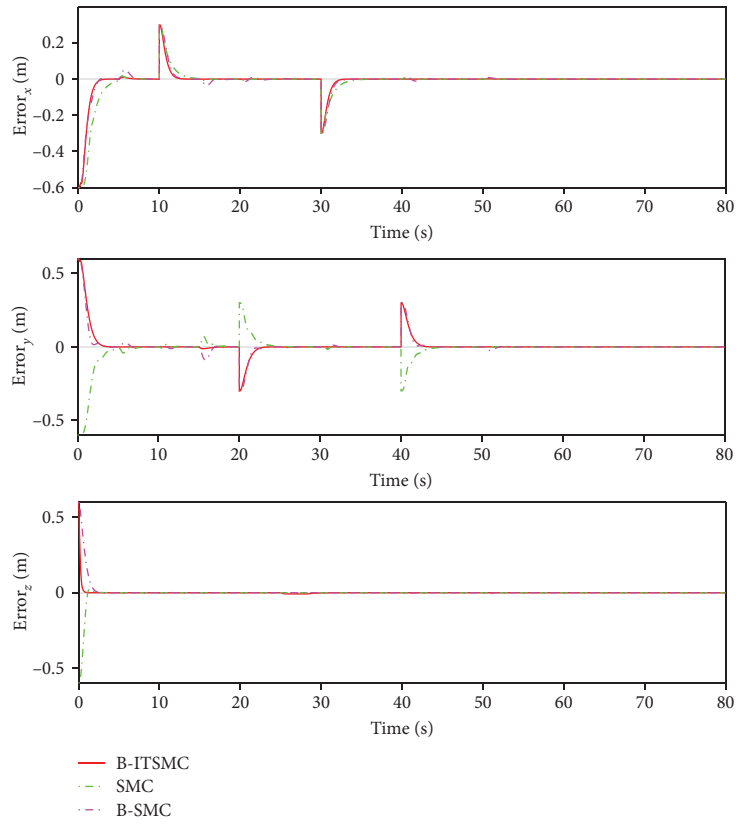

Figure 5: Position errors.

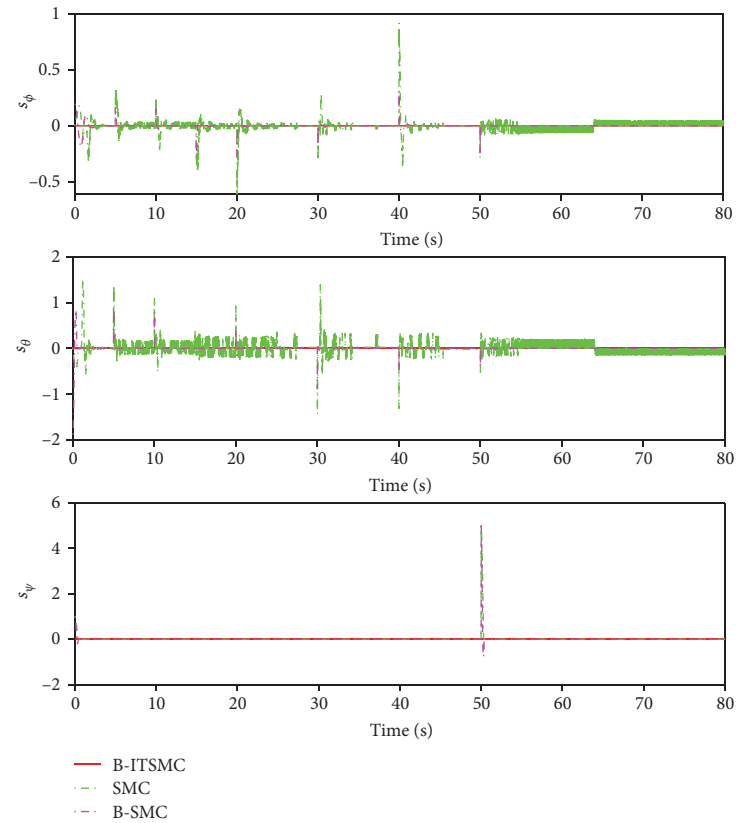

Figure 6: Tracking errors (s_ϕ, s_θ, and s_ψ), B-ITSMC.

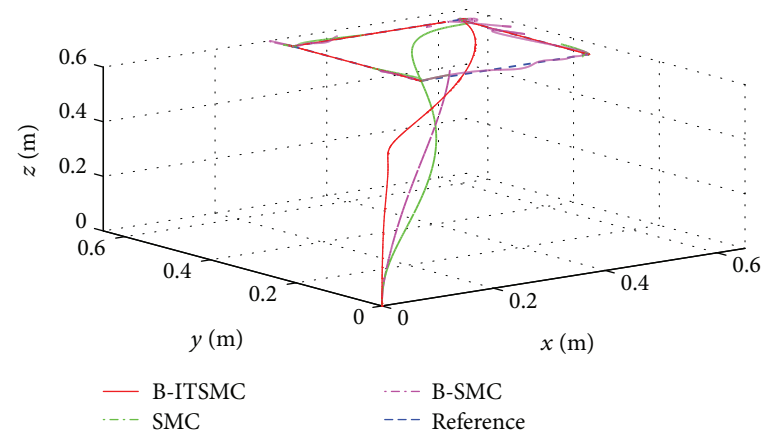

Figure 7: Flight trajectory tracking, B-RITSMC.

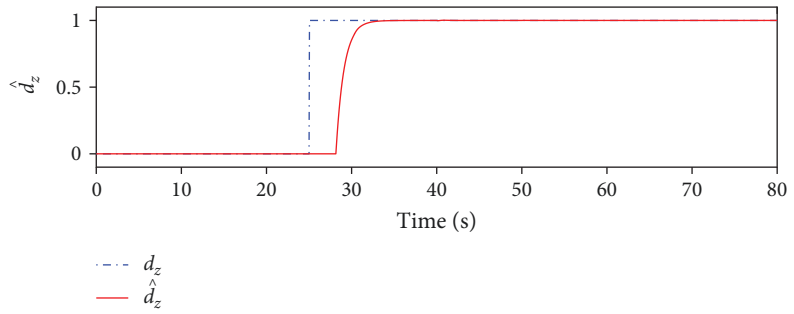

Figure 8: The estimate of the d_z parameter.

5. Conclusions

In this study, we have examined the problem of the flight trajectory-tracking phenomenon of the quadrotor with disturbances. The proposed control scheme is made up of three different parts: control of an altitude, a horizontal position, and an attitude subsystem. Firstly, the altitude subsystem is addressed based on adaptive backstepping. Also, the backstepping technique is designed to control the positions x and y of a quadrotor. The control objectives of this loop are (i) obtaining the desired roll and pitch angles, (ii) tracking the desired flight trajectory in finite time, and (iii) generating the total thrust. Secondly, a new robust integral terminal sliding mode controller has been constructed to stabilize the attitude subsystem. The objectives of the RITSMC control scheme are

(i) tracking the desired angles

(ii) stabilizing the quadrotor attitude

(iii) generating the rolling, pitching, and yawing torques

In addition, the proposed controller achieves the fast and accurate tracking of the quadrotor trajectory. Finally, simulation results have demonstrated that the proposed controller is able to improve control performance of the quadrotor UAV system in the presence of external disturbances. The proposed control strategy has shown the effectiveness and superiority of the classical sliding mode control strategy and backstepping sliding mode control technique.

The following points will be addressed in the future work:

(i) Taking into account the motor dynamics of the quadrotor

(ii) Inclusion of a fault detection in the actuators and sensors

(iii) Use of adaptive RITSMC approach in the improvement of the quadrotor control system

Data Availability

No new data were created during the study.

Conflicts of Interest

The authors declare that they have no conflicts of interest.

References

[1] M. Hassanalian and A. Abdelkefi, "Classifications, applications, and design challenges of drones: a review," *Progress in Aerospace Science*, vol. 91, pp. 99–131, 2017.

[2] A. Mairaj, A. I. Baba, and A. Y. Javaid, "Application specific drone simulators: recent advances and challenges," *Simulation Modelling Practice and Theory*, vol. 94, pp. 100–117, 2019.

[3] H. Mo and G. Farid, "Nonlinear and adaptive intelligent control techniques for quadrotor UAV - a survey," *Asian Journal of Control*, vol. 21, no. 2, pp. 989–1008, 2018.

[4] N. Wang, Q. Deng, G. Xie, and X. Pan, "Hybrid finite-time trajectory tracking control of a quadrotor," *ISA Transactions*, vol. 90, pp. 278–286, 2019.

[5] Z. Li, X. Ma, and Y. Li, "Robust tracking control strategy for a quadrotor using RPD-SMC and RISE," *Neurocomputing*, vol. 331, pp. 312–322, 2019.

[6] A. A. Najm and I. K. Ibraheem, "Nonlinear PID controller design for a 6-DOF UAV quadrotor system," *Engineering Science and Technology, an International Journal*, 2019.

[7] M. Vahdanipour and M. Khodabandeh, "Adaptive fractional order sliding mode control for a quadrotor with a varying load," *Aerospace Science and Technology*, vol. 86, pp. 737–747, 2019.

[8] F. Chen, R. Jiang, K. Zhang, B. Jiang, and G. Tao, "Robust backstepping sliding-mode control and observer-based fault estimation for a quadrotor UAV," *IEEE Transactions on Industrial Electronics*, vol. 63, no. 8, pp. 5044–5056, 2016.

[9] E. H. Zheng, J. J. Xiong, and J. L. Luo, "Second order sliding mode control for a quadrotor UAV," *ISA Transactions*, vol. 53, no. 4, pp. 1350–1356, 2014.

[10] J. J. Xiong and G. B. Zhang, "Global fast dynamic terminal sliding mode control for a quadrotor UAV," *ISA Transactions*, vol. 66, pp. 233–240, 2017.

[11] S. Mobayen and F. Tchier, "Nonsingular fast terminal sliding-mode stabilizer for a class of uncertain nonlinear systems based on disturbance observer," *Scientia Iranica*, vol. 24, no. 3, pp. 1410–1418, 2017.

[12] O. Mofid and S. Mobayen, "Adaptive sliding mode control for finite-time stability of quad-rotor UAVs with parametric uncertainties," *ISA Transactions*, vol. 72, pp. 1–14, 2018.

[13] Z. Jia, J. Yu, Y. Mei, Y. Chen, Y. Shen, and X. Ai, "Integral backstepping sliding mode control for quadrotor helicopter under external uncertain disturbances," *Aerospace Science and Technology*, vol. 68, pp. 299–307, 2017.

[14] C. C. Hua, K. Wang, J. N. Chen, and X. You, "Tracking differentiator and extended state observer-based nonsingular fast terminal sliding mode attitude control for a quadrotor," *Nonlinear Dynamics*, vol. 94, no. 1, pp. 343–354, 2018.

[15] S. Amirkhani, S. Mobayen, N. Iliaee, O. Boubaker, and S. H. Hosseinnia, "Fast terminal sliding mode tracking control of nonlinear uncertain mass–spring system with experimental verifications," *International Journal of Advanced Robotic Systems*, vol. 16, no. 1, 2019.

[16] F. Muñoz, E. S. Espinoza, I. González-Hernández, S. Salazar, and R. Lozano, "Robust trajectory tracking for unmanned aircraft systems using a nonsingular terminal modified super-twisting sliding mode controller," *Journal of Intelligent & Robotic Systems*, vol. 93, no. 1-2, pp. 55–72, 2019.

[17] D. Ashtiani Haghighi and S. Mobayen, "Design of an adaptive super-twisting decoupled terminal sliding mode control scheme for a class of fourth-order systems," *ISA Transactions*, vol. 75, pp. 216–225, 2018.

[18] J. J. Xiong and E. H. Zheng, "Position and attitude tracking control for a quadrotor UAV," *ISA Transactions*, vol. 53, no. 3, pp. 725–731, 2014.

[19] S. Bouabdallah and R. Siegwart, "Backstepping and sliding-mode techniques applied to an indoor micro quadrotor," in *Proceedings of the 2005 IEEE International Conference on Robotics and Automation*, pp. 2247–2252, Barcelona, Spain, April 2005.

[20] H. Liu, J. Xi, and Y. Zhong, "Robust attitude stabilization for nonlinear quadrotor systems with uncertainties and delays," *IEEE Transactions on Industrial Electronics*, vol. 64, no. 7, pp. 5585–5594, 2017.

[21] M. Labbadi, M. Cherkaoui, Y. El Houm, and M. Guisser, "A comparative analysis of control strategies for stabilizing a quadrotor," in *Information Systems and Technologies to Support Learning. EMENA-ISTL 2018. Smart Innovation, Systems and Technologies*, Á. Rocha and M. Serrhini, Eds., vol. 111 of Smart Innovation, Systems and Technologies, Springer, Cham, 2019.

[22] M. Labbadi, M. Cherkaoui, Y. El Houm, and M. Guisser, "Modeling and robust integral sliding mode control for a quadrotor unmanned aerial vehicle," in *2018 6th International Renewable and Sustainable Energy Conference (IRSEC)*, pp. 1–6, Rabat, Morocco, December 2018.

[23] R. Zhang, L. Dong, and C. Sun, "Adaptive nonsingular terminal sliding mode control design for near space hypersonic vehicles," *IEEE/CAA Journal of Automatica Sinica*, vol. 1, no. 2, pp. 155–161, 2014.

[24] A. Riani, T. Madani, A. Benallegue, and K. Djouani, "Adaptive integral terminal sliding mode control for upper-limb rehabilitation exoskeleton," *Control Engineering Practice*, vol. 75, pp. 108–117, 2018.

[25] F. P. Freire, N. A. Martins, and F. Splendor, "A simple optimization method for tuning the gains of PID controllers for the autopilot of Cessna 182 aircraft using model-in-the-loop platform," *Journal of Control, Automation and Electrical Systems*, vol. 29, no. 4, pp. 441–450, 2018.